

Electrodeposited Submicron Thermocouples with Microsecond Response Times

M. E. Bourg,[†] W. E. van der Veer,[†] A. G. Grüell,[‡] and R. M. Penner^{*,†}

Department of Chemistry and Institute for Surface and Interface Science, University of California, Irvine, California 92697-2025, and Department of Physical Chemistry, The University of Barcelona, Martí i Franquès 1, E-08028 Barcelona, Spain

Received August 9, 2007; Revised Manuscript Received August 31, 2007

ABSTRACT

We describe a procedure for preparing submicron scale silver–nickel thermocouples (TCs) using electrochemical step edge decoration on graphite surfaces. Each fabrication operation produced ensembles of 2–20 TCs with diameters in the 1.0 μm to 500 nm range. These “sub- μm TCs” (SMTCs) produced linear voltage versus temperature output over the range from 20 to 100 °C characterized by a Seebeck coefficient of $20 \pm 1 \mu\text{V}/^\circ\text{C}$, equal to the $21 \mu\text{V}/^\circ\text{C}$ that is theoretically expected for a junction between these two metals. The time response of SMTCs was evaluated using two different laser-heating methods and compared with the smallest mechanically robust commercially available type J TCs. Electrochemical etching of the silver wire introduced constrictions at grain boundaries that reduced the thermal mass of the junction without altering its integrity or its overall diameter, producing a decrease of the measured rise time for SMTCs up to 96%.

To understand processes such as turbulent combustion and detonation and to achieve real time monitoring of these processes within internal combustion engines for example, temperature measurements with a time resolution in the submicrosecond range are required. The smallest commercially available thermocouples have time responses in the millisecond range. Faster response times (Table 1) have been achieved by forming junctions using evaporated metal films. Measurements on such thin-film thermocouples (TFTCs) have exposed a serious problem: the response times of TFTCs are directly proportional to the total thickness of the metal films, and a response time of 1.0 μs or less requires films that are less than 100 nm in thickness (Table 1). For such TFTCs, the Seebeck coefficient, which is the slope of the output voltage versus temperature response function, is depressed relative to its value for macroscopic junctions of the same two metals.^{1–6} The resulting loss of sensitivity for the TFTC can be as high as 85% (Table 1). The Seebeck coefficient is depressed because the thermopower of metal films decreases in proportion to $1/t$ as the thickness, t , is reduced.^{1–6} Unavoidably for TFTCs, temperature sensitivity must be traded off for improved response time.

Thermocouples based upon submicron diameter wires (SMTCs) contend with the same physics as TFTCs, but the thermal mass of a cylindrical wire is proportional to the (radius)² with the result being that response times decrease

faster with decreasing size than is the case for TFTCs. Does this mean that SMTCs can achieve microsecond response times without sacrificing sensitivity? The answer to this question is not known; in spite of the technological maturity of TCs and resistance temperature detectors (RTDs), versions of these devices based upon submicron wires have not been evaluated to our knowledge. We take a first step in this direction in this paper, which has three objectives: (1) To describe an unconventional approach for fabricating silver–nickel thermocouples that are smaller than 1.0 μm in diameter, (2) to measure the temporal properties of SMTCs for measuring temperature, and (3) to measure the Seebeck coefficients of the SMTCs.

Ensembles of 2–20 Ag/Ni SMTCs were fabricated using the process shown in Figure 1. Step edges naturally present on highly oriented pyrolytic graphite (HOPG) crystals were used to template the growth of submicron silver wires (blue) and then nickel wires (gray) in separate steps using the electrochemical step edge decoration method described previously.^{7,8} By starting with a freshly cleaved (0001)-oriented HOPG crystal, half of the deposition area of the HOPG surface was masked using Crystalbond, an acetone-soluble masking agent (Ted Pella, Cat. 821–1), by melting it directly on a HOPG surface heated on a hot plate (Figure 1, step 1). Then in step 2, silver wires with a diameter of 500 nm to 1.0 μm were electrodeposited on unmasked regions of the surface from a solution containing 1 mM Ag_2SO_4 (Sigma Aldrich, 99.999%), 1 mM saccharin (Alfa

* Corresponding author. E-mail: rmpenner@uci.edu.

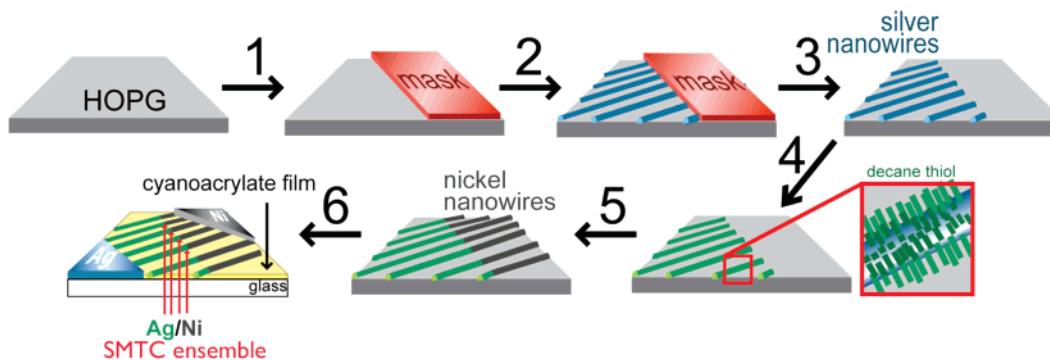
[†] University of California.

[‡] The University of Barcelona.

Table 1: Thermocouples and a RTD^a with Rapid Response Characteristics

corresponding author	technology	slope, $\mu\text{V}/^\circ\text{C}$ (% of bulk)	response time, μs	ref
M. Tagawa	cold wire ^b	n/a	11	10
J.P. Prenel	thin film TC ^c	4.4 ± 0.6 (35%)	1.0 ± 0.1	11
E. Schreck	thin film TC ^d	7 (33%)	250	12
B. Revaz	thin film TC ^e	6 (38%)	200	13
A. Lewis	micropipette-based submicrometer TC ^f	7 (40%)	1	14
F.W. Pease K.E. Goodson	thin film TC ^g	2.9 ± 0.6 (14%)	0.30 ± 0.03	15
X. Li	thin film TC ^h	28 (68%)	0.040	16
this work	etched, $\approx 1.0 \mu\text{m}$ diameter electrodeposited Ag/Ni thermocouple	20 ± 1 (95%)	0.14 ± 0.05 to 3.3 ± 0.1	

^a RTD = resistance temperature detector. ^b An RTD consisting of a suspended $0.63 \mu\text{m}$ diameter platinum wire. The time constant was taken to be the $1/f$ evaluated at the frequency at which the maximum voltage output, $V_{\text{out,max}}$, was attenuated by 0.95. ^c The thermocouple was composed of $>200 \text{ nm}$ thick Au and Pd films on glass. An Ar ion laser at $\lambda_{\text{ex}} = 514 \text{ nm}$ and 52 mW , chopped at 200 Hz , was used to investigate the time response. The time constant was taken as the time required to reach 95% of the maximum voltage output, $V_{\text{out,max}}$. ^d A thermocouple composed of a $4 \mu\text{m}$ thick, 80 nm wide Ni film, and a 200 nm thick Au film embedded in alumina. A $50 \mu\text{s}$ heat pulse from a resistive heater was used to investigate the time response. The time constant was taken to be the time to reach $0.90 V_{\text{out,max}}$. ^e A thermocouple composed of a 200 nm Au film and a 500 nm Pd film on a polyimide-coated steel foil. Response time was investigated using a $104 \mu\text{s}$ 116 W discharge from an electron discharge machine (EDM). The reported time constant was the time elapsing between $0.1 V_{\text{out,max}}$ and $0.9 V_{\text{out,max}}$. ^f A thermocouple composed of a Au-coated glass micropipette with a Pt core. The tip diameter was $1 \mu\text{m}$. A Q-switched Nd:YAG laser, $1.064 \mu\text{m}$, 300 ns pulse width, 1 mJ , and 100 Hz repetition rate were used to investigate the time response. The reported time constant is the time required for V_{out} to decay with cooling to 63% of its $V_{\text{out,max}}$ after the application of a laser pulse. ^g A thermocouple composed of a 50 nm thick Au film and a 30 nm thick Ni film on silicon oxide. The thermocouple is covered by poly(methyl methacrylate). A Nd:YAG laser with a 10 ns pulse width was used to investigate the time response. The reported time constant was the time elapsing between $0.1 V_{\text{out,max}}$ and $0.9 V_{\text{out,max}}$. ^h A thermocouple comprised of a 45 nm alumel film and a 30 nm chromel film on an insulating layer composed of Al_2O_3 and Si_3N_4 and embedded in Ni. A Q-switched Nd:YAG laser, 355 nm , 10 ns pulse width, and a 20 Hz repetition rate, was used to investigate the time response. The reported time constant was the time elapsing between $0.1 V_{\text{out,max}}$ and $0.9 V_{\text{out,max}}$.

**Figure 1.** Six step process flow for fabrication of Ag/Ni submicron thermocouple ensembles by electrochemical step edge decoration.

Aesar, 98+%), and $0.1 \text{ M Na}_2\text{SO}_4$ (Fisher, Enzyme Grade), and the pH was adjusted to 1.0 with H_2SO_4 (JT Baker, Ultratex II). The potential program employed for silver wire growth was the following: $+1.1 \text{ V}$ for 5 s , -0.8 V for 50 ms , and -0.18 V for 900 s , all versus a silver wire reference electrode. The Crystallbond mask was then completely removed by exhaustively rinsing the surface in acetone (EMD, HPLC grade) five times in succession, followed by rinses in HPLC-grade methanol, isopropanol, water (Millipore, $\rho = 18.2 \text{ M}\Omega \text{ cm}$), and ethanol. In step 4, the silver wires were coated with a self-assembled monolayer (SAM) of 1-decanethiol (TCI America, 98%) from a 2 mM solution in ethanol (Gold Shield, 200 proof). Then, in step 5, nickel

wire segments were electrodeposited in the previously masked region by electrodeposition from a solution of $5 \text{ mM NiCl}_2 \cdot 6\text{H}_2\text{O}$ (Acros Organics, 99.9999%), $3 \text{ mM NiSO}_4 \cdot 6\text{H}_2\text{O}$ (Aldrich, 99%), $0.01 \text{ M H}_3\text{BO}_3$ (Acros Organics, 99.99%), and $0.1 \text{ M Na}_2\text{SO}_4$ (Fisher, Enzyme Grade) using the following potential program: -1.0 V for 5 ms , -0.7 V for 600 s versus saturated calomel electrode. Finally, in step 6 the Ag/Ni SMTCs produced in steps 1–5 were transferred from the graphite surface onto a glass microscope slide by pressing the graphite surface on which the SMTCs were formed onto a drop of cyanoacrylate adhesive (Special T, Satellite City) and allowing it to harden for 12 h . Then the graphite was dislodged using a razor blade, and the SMTCs

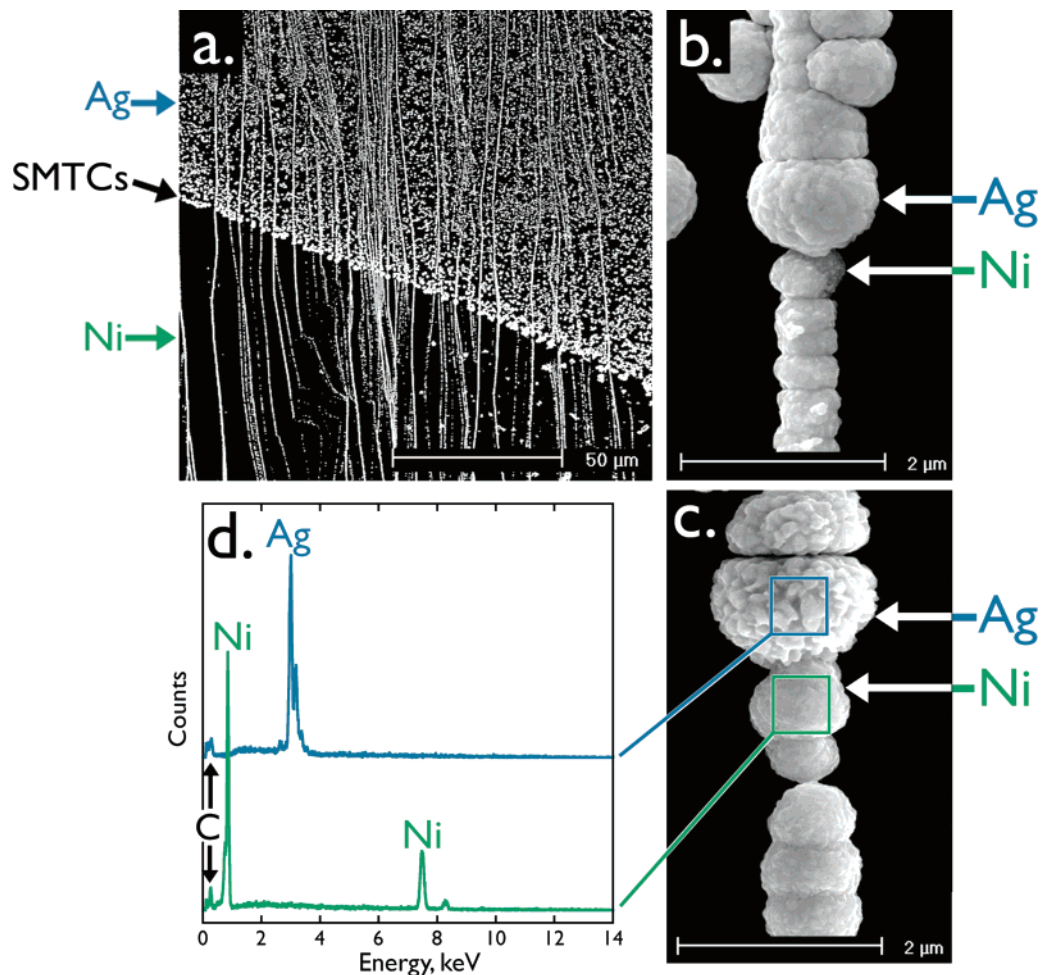


Figure 2. (a) Low magnification SEM image of an ensemble of Ag/Ni submicron junctions on HOPG. The wires grow on the step edges of the HOPG and therefore form parallel arrays. At the interface of the Ag/Ni junctions, the Ag particles are large, 500 nm to 1 μm , but the diameter of these wires tapers with increasing distance from this compositional interface. (b) High-magnification SEM image of a single Ag/Ni junction. (c) A high-magnification SEM image of a single etched Ag/Ni junction. (d) EDX microanalysis spectra for both the Ag and Ni wires. The absence of Ni peaks in the spectrum for the Ag wire (blue) confirms that the *n*-alkanethiol SAM effectively insulates the Ag segment from contact with the nickel-plating solution. The carbon (C) peak seen in both the Ag (blue) and Ni (green) spectra is from the HOPG substrate.

remained embedded in an ≈ 1 cm diameter cyanoacrylate disk on the glass surface. Electrical contacts to an unknown number of deposited SMTCs were prepared using nickel- (MG Chemicals, Cat. 840-20g) and silver- (Ted Pella Cat. 16032) painted current collectors on the corresponding two sides of the junction. The distance between these current collectors was 300 μm on average, but this distance was not precisely controlled.

Some SMTCs were also subjected to an additional processing step that involved etching of the silver wires. Etching involved the application of 1 μA of anodic current for 1000 s immediately after silver deposition in step 2. This process materially affected the performance of SMTCs as described below. Our success rate for obtaining functioning SMTCs using this approach was 80%, start to finish, with virtually all failures occurring at the contacts, not the electrochemically “welded” junctions. Etched and nonetched SMTCs withstood repeated testing over a period of several months with storage in laboratory air.

The interface between silver (top) and nickel (bottom) regions is shown at low magnification in the scanning

electron microscopy (SEM) image of Figure 2a. The vertical lines seen in this image are step edges that have been decorated with continuous silver or nickel wires. Upon closer inspection of this SEM image, it is apparent that the wires remain continuous as they cross the Ag/Ni compositional interface. In addition to wires, particles composed of silver (by energy dispersive X-ray (EDX)) are also present in the silver-deposited region (Figure 2a, top). These particles do not degrade the properties of the Ag/Ni junctions that are formed during this process because they are not electrically continuous with the silver wires present on step edges. Junctions between silver and nickel wire segments are shown at high magnification in the SEMs of Figure 2b,c. A typical “as-prepared” SMTC junction is shown in Figure 2b, whereas 2c shows a junction that was subjected to etching as described above. Etching did not significantly reduce the overall diameter of the junctions that were formed, but it did produce deeper grain boundaries along the wire axes on the silver side of the junction and it often introduced constrictions that materially affected the performance of these junctions as thermocouples (see below). It is important to

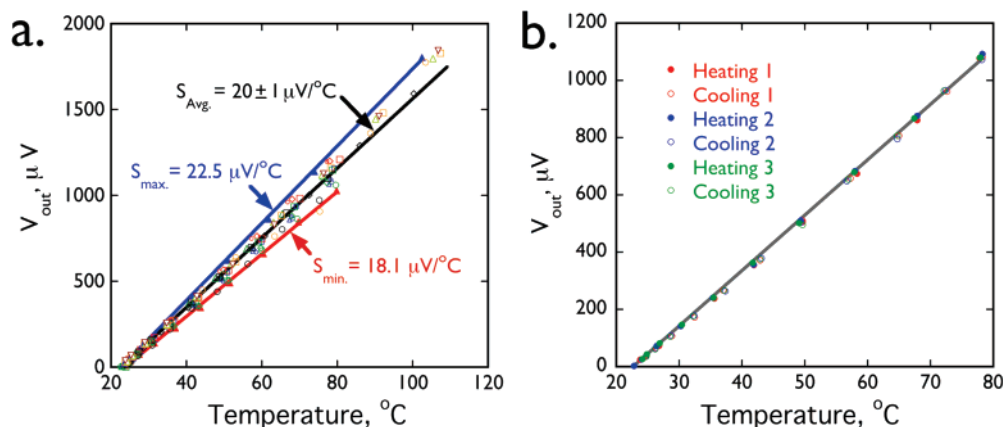


Figure 3. (a) Heating calibration for 20 Ag/Ni SMTCs. The mean sensitivity measured was $20.4 \pm 1.2 \mu\text{V } ^\circ\text{C}^{-1}$, and it ranged from a minimum of $18.1 \mu\text{V } ^\circ\text{C}^{-1}$ to a maximum of $22.5 \mu\text{V } ^\circ\text{C}^{-1}$. (b) Heating and cooling curves showing the absence of hysteresis over three cycles. The heating rate here was approximately $0.018 \text{ } ^\circ\text{C sec}^{-1}$, while the cooling rate was $0.016 \text{ } ^\circ\text{C sec}^{-1}$.

note that the *n*-alkane thiol SAM passivation of the silver wires in step 4 completely suppressed nickel electrodeposition on these wires in step 5. We base this conclusion on EDX microanalysis spectra acquired on either side of these junctions before transfer off the HOPG. A typical pair of these spectra, Figure 2d, shows clean silver and nickel surfaces immediately adjacent to one another for the junction shown in Figure 2c.

As shown in Figure 3a, for eight different SMTCs the output voltage versus temperature was linear from 20 to 100 °C. No detectable hysteresis in these data was discernible in these measurements (Figure 3b). The slope of the plots shown in Figure 3a equals the Seebeck coefficient, *S*, which ranged from 18 to 23 $\mu\text{V}/^\circ\text{C}$ with $S_{\text{ave}} = 20 \pm 1 \mu\text{V}/^\circ\text{C}$ for 20 devices.

Among these 20 SMTCs, *S* ranged from 9.5% higher to 14% lower than the expected bulk value of *S* for these 2 metals of $21 \mu\text{V}/^\circ\text{C}$. The high values for *S* seen here are not surprising based on the dimensions of these wire junctions seen in Figure 2b,c; the minimum diameters of the Ag/Ni junctions prepared here were in the 200 nm range, which is well above the threshold of $\approx 100 \text{ nm}$ at which size-induced depression of *S* has been seen for TFTCs (cf. refs 2,4–6). Can such SMTCs compete in terms of time response with TFTCs in which the films are 100 nm in thickness or less?

This question cannot be answered definitively because the measured time response depends critically on the method used to measure it including the laser wavelength, its power, and the pulse duration, and no standardized methodology for this measurement exists to our knowledge. We therefore measured the temporal response properties of these SMTCs using two different laser-heating methods and compared these devices with two commercial bare wire thermocouples (Omega, Type J, Iron-Constantan) with diameters of 75 (Model IRCO 003) and 125 μm (Model IRCO 005). Like the SMTCs, these commercial TCs were mounted in a cyanoacrylate film on glass.

The steady-state response of SMTC ensembles to pulsed laser heating on the 0.25–50 ms time scale was assessed by exposing these devices to chopped laser heating from a continuous wave (CW) argon ion laser that produced

350 mW (unchopped) at $\lambda_{\text{ex}} = 514 \text{ nm}$. The chopping frequency varied from 20 Hz to 3.9 kHz. The amplitude of the steady-state thermocouple output was measured by amplifying the TC output and displaying the voltage versus time transients on an oscilloscope. Typical traces acquired in this way at 20 Hz and 1.8 kHz (Figure 4b,c, respectively) for a SMTC ensemble and a 75 μm type J TC show that the voltage output of both devices is strongly modulated at 20 Hz (Figure 4b). The voltage excursions seen here correspond to a change in temperature of $0.4 \text{ } ^\circ\text{C}$ in the case of the type J TC ($22 \mu\text{V} \div 52 \mu\text{V}/^\circ\text{C}$) and $2.4 \text{ } ^\circ\text{C}$ in the case of the SMTC ensemble ($50 \mu\text{V} \div 21 \mu\text{V}/^\circ\text{C}$). Larger temperature modulations for SMTCs versus the 75 μm type J TC were systematically observed in nine experiments and may reflect the lower thermal mass of the SMTCs ensembles. Above 500 Hz, no detectable voltage modulation could be observed for the type J TCs, but SMTCs continued to show modulated voltage responses up to 3 kHz (a comparison at 1.8 kHz is shown in Figure 4c). Plots of the output voltage amplitude, V_{out} , normalized by the amplitude at 20 Hz ($V_{\text{out},20 \text{ Hz}}$) as a function of chopping frequency allow the performance of the type J TCs, unetched SMTCs, and etched SMTCs to be differentiated (Figure 4 d,e). The degree to which $V_{\text{out}}/V_{\text{out},20 \text{ Hz}}$ is attenuated as a function of frequency can be taken to be an indication of the relative temporal responses of these three types of devices. Comparing the frequency for which $V_{\text{out}}/V_{\text{out},20 \text{ Hz}} = 0.05$, for example (Figure 4e), we obtain values of 174 ± 2 , 700 ± 200 , and $2000 \pm 200 \text{ Hz}$ for the 75 μm type J TC, unetched SMTCs, and etched SMTCs, respectively.

Why are the etched junctions faster? The Ag/Ni junction is strongly thermally coupled to the solid metal wires on either side of the junction, and it is well established⁹ that the transport of heat into these connecting wire segments contributes to the total thermal mass of the junction. In the specific case of Ag/Ni, the thermal coupling is stronger in the silver direction since the thermal conductivity of the silver wire is more than four times that of nickel (429 vs. 91 W/(m K)). The constrictions in the silver wires that are introduced by etching apparently impede thermal transport in the silver direction thereby thermally decoupling the Ag/Ni junction.

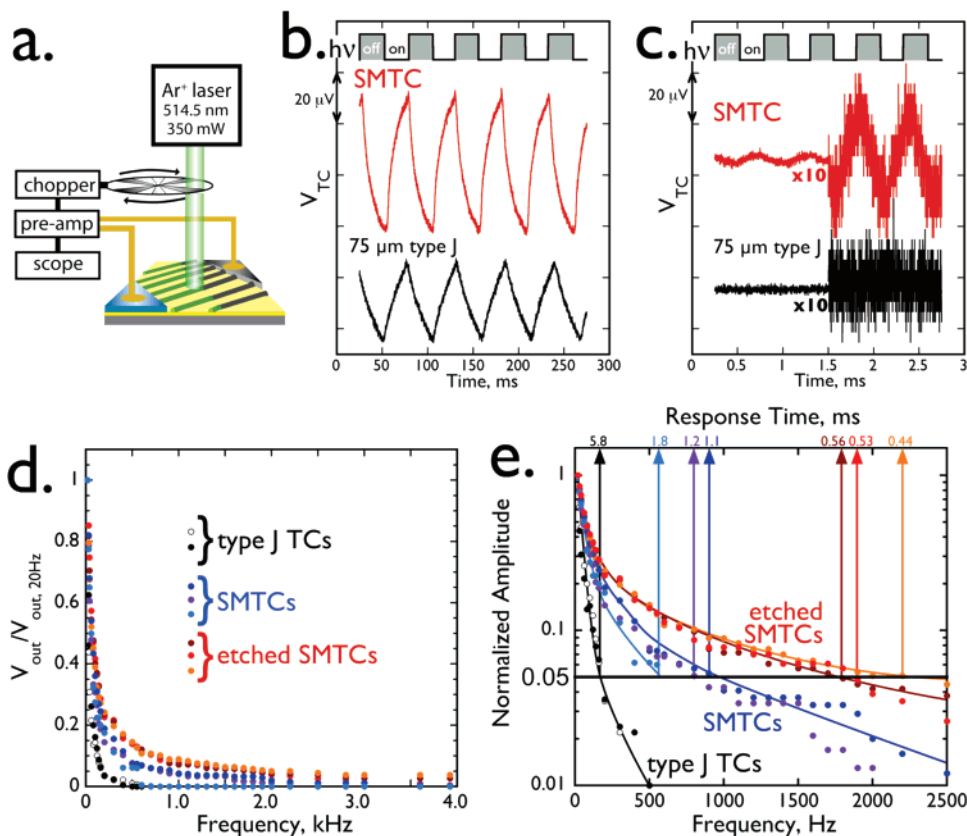


Figure 4. (a) Schematic diagram of the response time measurement system. A CW Ar ion laser ($\lambda_{\text{ex}} = 514 \text{ nm}$, beam diameter = 2 mm, power = 350 mW) was used to heat the Ag/Ni SMTC. A mechanical chopper (Stanford Research Systems, SR40) was used to modulate this laser fluence. The thermocouple output, V_{out} , was amplified (Stanford Research Systems, SR560 voltage preamplifier) and the transient was recorded on an oscilloscope (Tektronix, TDS 1012). (b) V_{out} versus time traces obtained at a chopping frequency of 20 Hz for a Ag/Ni SMTC and a $75 \mu\text{m}$ type J TC. (c) V_{out} versus time traces for the same TCs shown in (b) but at a chopping frequency of 1800 Hz. (d) Plot of V_{out} normalized to output voltage at 20 Hz, $V_{\text{out},20 \text{ Hz}}$, versus the chopping frequency for 75 and 125 μm type J TCs, Ag/Ni SMTCs, and etched Ag/Ni SMTCs. (e) Log-normal plot of the same data shown in (c). The response time was defined as the time ($1/f$) when the signal was attenuated to $V_{\text{out}}/V_{\text{out},20 \text{ Hz}} = 0.05$.

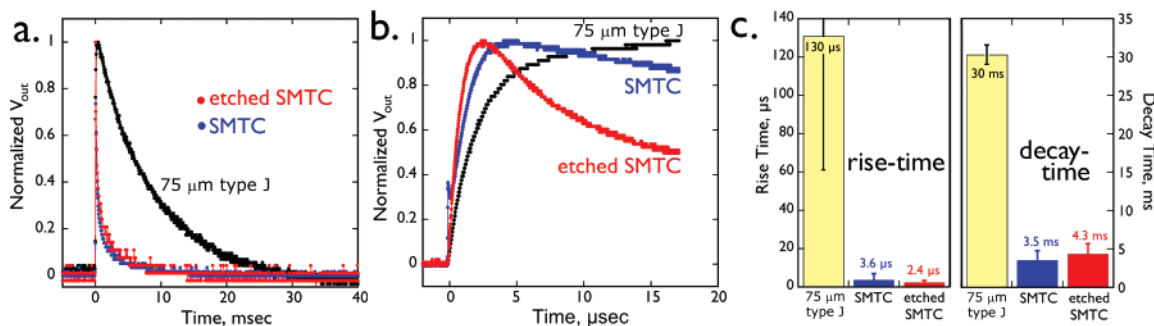


Figure 5. (a) Normalized voltage transients for a $75 \mu\text{m}$ type J TC, a Ag/Ni SMTC, and an etched Ag/Ni SMTC obtained from a 7 ns pulse from a Nd:YAG laser with $\lambda_{\text{ex}} = 532 \text{ nm}$ and a peak power density of 0.57 MW/cm^2 . (b) The short time behavior of the transients shown in (a). (c) Plot of the average rise times (left) and decay times (right) for $75 \mu\text{m}$ type J TCs, Ag/Ni SMTCs, and etched Ag/Ni SMTCs. The rise time was defined as the time necessary to obtain 90% of the maximum V_{out} , and the decay time was defined as the time required for the signal to decay to 10% of the maximum V_{out} .

In the steady-state measurement just described, heating and cooling occur with the same apparent time constant (see Figures 4b,c), determined by a convolution of the rise time and the decay time for each device. These two time constants are not the same because they correspond to fundamentally different processes: laser heating of a cold TC junction and its surrounding matrix, and conductive, convective, and radiative heat dissipation from the TC and its heated

surroundings into the cold contacting matrix in which it is mounted. A deconvolution of these two time constants is possible using an experiment in which the TC is first heated by a laser pulse having a duration that is much shorter than the time constant of the TC, and the rate of cooling can be observed from the heated state for an extended time period. We approximated this experiment using light from a frequency-doubled Continuum Surelite I Nd:Yag laser at λ_{ex}

= 532 nm. The duration of these pulses was 7 ns, the beam diameter was 8 mm, and the peak power density at the TC was 0.57 MW/cm². The response of each TC was measured as a current using a fast transimpedance amplifier (National LMH6624) that reduced the total resistance and minimized the RC (product of the resistance in ohms and the capacitance in farads) time constant of this circuit. The measured current could be directly related to the V_{out} of the TC using the time-independent TC resistance but we report here (Figure 5) just the voltage output of this circuit, which is proportional to V_{out} .

Normalized temperature transients measured in this way (Figure 5a,b) show rise times for as-prepared and etched SMTCs of 4 ± 3 and 2 ± 1 μs averaged over 4–5 devices of each type, compared with a 130 ± 70 μs for the 75 μm type J TC. As is apparent in Figure 5a,b, decay times were much slower (in the 3–4 ms time range for SMTCs compared with 30 ms for the 75 μm type J TC). The intrinsic heterogeneity of these SMTCs, however, produced a relatively broad range of response times for different devices with rise times, for example, ranging from 140 ± 5 ns to 3.3 ± 0.1 μs . The devices at the lower end of this range are among the fastest TCs of any type reported to date (Table 1). However, SMTCs devices operating at the lower end of this range could not be reproducibly fabricated, and this constitutes a clear deficiency of this fabrication methodology. This deficiency can be traced to a lack of precision in the electrodeposition of the smallest possible silver and nickel wires on the HOPG surface. Despite this issue, the data presented here collectively demonstrates that SMTCs can alleviate an important shortcoming of TFTCs, specifically, the loss of temperature measurement sensitivity with decreasing device time response. These results provide motivation to produce thermocouples using wires in the nanometer range and to probe the wire diameter-dependence of the TC sensitivity for these devices. Achieving this objective will require a nanofabrication methodology having a higher degree of precision.

Acknowledgment. This work was funded by the National Science Foundation (Grant CHE-0641169) and the Petroleum Research Fund of the American Chemical Society (Grant 46815-AC10). A.G.G. gratefully acknowledges economical support from the Department of Universities, Research and Information Society (DURSI) of the Catalonia Government through Grant 2005-BE-00730. Graphite for this work was supplied by a grant from the EU Commission FP6 NMP-3 project 505457-1 ULTRA-1D.

References

- (1) Walter, E.; Murray, B.; Favier, F.; Penner, R. *Adv. Mater.* **2003**, *15*, 396.
- (2) Chopra, K. L.; Bahl, S. K.; Randlett, M. R. *J. Appl. Phys.* **1968**, *39*, 1525.
- (3) Rowe, D. M. *CRC Handbook of Thermoelectrics*; CRC Press: Washington D.C., 1995; p 687.
- (4) Jain, G. C.; Verma, B. S. *Thin Solid Films* **1973**, *15*, 191.
- (5) Salvadori, M. C.; Vaz, A. R.; Teixeira, F. S.; Cattani, M.; Brown, I. G. *Appl. Phys. Lett.* **2006**, *88*, 133106/1.
- (6) Scarioni, L.; Castro, E. M. *J. Appl. Phys.* **2000**, *87*, 4337.
- (7) Walter, E. C.; Murray, B. J.; Favier, F.; Kaltenpoth, G.; Grunze, M.; Penner, R. M. *J. Phys. Chem. B* **2002**, *106*, 11407.
- (8) Walter, E. C.; Zach, M. P.; Favier, F.; Murray, B. J.; Inazu, K.; Hemminger, J. C.; Penner, R. M. *ChemPhysChem.* **2003**, *4*, 131.
- (9) Fralick, G. C.; Forney, L. J. *Rev. Sci. Instrum.* **1993**, *64*, 3236.
- (10) Tagawa, M.; Kato, K.; Ohta, Y. *Rev. Sci. Instrum.* **2005**, *76*, 1.
- (11) Serio, B.; Nika, P.; Prenel, J. P. *Rev. Sci. Instrum.* **2000**, *71*, 4306.
- (12) Schreck, E.; Hiller, B.; Singh, G. P. *Rev. Sci. Instrum.* **1993**, *64*, 218.
- (13) Revaz, B.; Fluekiger, R.; Carron, J.; Rappaz, M. *Sens. Actuators, A* **2005**, *A118*, 238.
- (14) Fish, G.; Bouevitch, O.; Kokotov, S.; Lieberman, K.; Palanker, D.; Turovets, I.; Lewisa, A. *Rev. Sci. Instrum.* **1995**, *66*, 3300.
- (15) Chu, D.; Bilir, D. T.; Pease, R. F. W.; Goodson, K. E. In *Thin film nano thermocouple sensors for applications in laser and electron beam irradiation*; 12th International Conference on Solid State Sensors, Actuators, and Microsystems, IEEE: Boston, 2003; p 1112–5.
- (16) Zhang, X.; Choi, H.; Datta, A.; Li, X. *J. Micromech. Microeng.* **2006**, *16*, 900.

NL071990Q